Table 1. *Maximum reduced rotation angles, longest Rodrigues vectors, restrictions for Rodrigues vectors and range of rotation axes for any combination of two symmetries*

Lattice symmetries	Maximum reduced rotation angle	Longest Rodrigues vector	Restrictions/range of rotation axes
Cubic	62·80	$(2^{1/2}-1, 2^{1/2}-1, 3-2\times2^{1/2})$	None / R^3
Hexagonal	93·84	$[(3^{1/2}-1), (3^{1/2}-1), (2-3^{1/2})]$	None / R^3
Tetragonal	98·42	$[1, (2^{1/2}-1), (2^{1/2}-1)]$	None / R^3
Orthorhombic	120	$(1, 1, 1)$	None / R^3
Cubic-cubic	62·80	$(2^{1/2}-1, 2^{1/2}-1, 3-2\times2^{1/2})$	$d_1 \geq d_2 \geq d_3 \geq 0$ / cubic SST*
Hexagonal-hexagonal	93·84	$[(3^{1/2}-1), (3^{1/2}-1), (2-3^{1/2})]$	$d_3 \geq 0, (1/3^{1/2})d_1 \geq d_2 \geq 0$ / hexagonal SST*
Tetragonal-tetragonal	98·42	$[1, (2^{1/2}-1), (2^{1/2}-1)]$	$d_3 \geq 0, d_1 \geq d_2 \geq 0$ / tetragonal SST*
Orthorhombic-orthorhombic	120	$(1, 1, 1)$	$d_i \geq 0, i = 1, 2, 3$ / orthorhombic SST*
Cubic-hexagonal	56·60	(x_0, x_6, x_4)	see § 8 / 1 + 2 octant of R^3 = double orthorhombic SST*
Cubic-tetragonal	62·80	$(2^{1/2}-1, 2^{1/2}-1, 3-2\times2^{1/2})$	1/8 of cubic / doubled tetragonal SST*
Cubic-orthorhombic	62·80	$(2^{1/2}-1, 2^{1/2}-1, 3-2\times2^{1/2})$	1/4 of cubic-cubic / doubled orthorhombic SST*
Hexagonal-tetragonal	90·98	$(1, x_4, x_4)$	see § 10 / doubled orthorhombic SST*
Hexagonal-orthorhombic	93·84	$[(3^{1/2}-1), (3^{1/2}-1), (2-3^{1/2})]$	1/4 of hexagonal-hexagonal / doubled orthorhombic SST*
Tetragonal-orthorhombic	98·42	$[1, (2^{1/2}-1), (2^{1/2}-1)]$	1/4 of tetragonal-tetragonal / doubled orthorhombic SST*

$x_0 = (2^{1/2}-1)$, $x_4 = (2\times2^{1/2}-3^{1/2}-1)/(3^{1/2}-1)$ and $x_6 = (2^{1/2}-3^{1/2}-6^{1/2}+3)/(3^{1/2}-1)$.

* SST = standard stereographic triangle.

References

BECKER, S. & PANCHANADEESWARAN (1989). *Text. Microstruct.* **10**, 167.

BIRSS, R. R. (1964). In *Symmetry and Magnetism*, edited by E. P. WOHLFARTH. London: North Holland.

BONNET, R. (1980). *Acta Cryst.* **A36**, 116–122.

BUNGE, H. J. (1982a). In *Quantitative Texture Analysis*, edited by C. ESLING & H. J. BUNGE. Oberursel: DGM.

BUNGE, H. J. (1982b). *Texture Analysis in Material Science.* London: Butterworth.

BUNGE, H. J. (1987). *Theoretical Methods of Texture Analysis.* Oberursel: DGM.

BUNGE, H. J. (1988). Proc. Int. Conf. on Texture of Materials 8 (ICOTOM-8), Santa Fé, USA, p. 69.

DUVAL, P. (1964). *Homographies, Quaternions and Rotations.* Oxford Univ. Press.

FRANK, F. C. (1987). Proc. Int. Conf. on Texture of Materials 8 (INCOTOM 8), Santa Fé, USA, pp. 3–13.

GERTSMAN, V. Y. (1989). Proc. Int. Conf. on Intergranular and Interface Boundaries, Paris, France, pp. C1-145–C1-150.

GRIMMER, H. (1974). *Acta Cryst.* **A30**, 685–688.

HAESSNER, F. & SCHRÖDER, G. (1977). *Z. Metallkd.* **68**, 624–635.

HANDSCOMB, D. C. (1958). *Can. J. Math.* **10**, 85–88.

HANSEN, J., POSPIECH, J. & LÜCKE, K. (1978). *Tables for Texture Analysis of Cubic Crystals.* Berlin: Springer.

HELMIG, K., MATTHIES, S. & VINEL, G. W. (1988). Proc. Int. Conf. on Texture of Materials 8 (ICOTOM-8), Santa Fé, USA, p. 55.

MACKENZIE, J. K. (1958). *Biometrika*, **45**, 229–240.

MATTHIES, S., HELMIG, K. & KUNZE, K. (1990). *Phys. Status Solidi B*, **157**, 71, 489.

MORRIS, R. & HECKLER, A. J. (1969). *Trans. Met. Soc. AIME*, **245**, 1877–1881.

NEUMANN, P. (1990). Proc. Int. Conf. on Texture of Materials 9 (INCOTOM 9), Avignon, France.

RODRIGUES, O. (1840). *J. Math. Pure Appl.* **5**, 380–440.

WAERDEN, B. L. VAN DER (1932). *Die Gruppentheoretische Methode in der Quantenmechanik.* Berlin: Springer.

Dynamical RHEED Calculations of Relaxation on Au(110)–2×1 Reconstruction

BY J. E. BONEVICH, Y. MA* AND L. D. MARKS

Department of Materials Science and Engineering, Northwestern University, Evanston, IL 60208, USA

(*Received* 23 *March* 1991; *accepted* 12 *June* 1991)

Abstract

Dynamical calculations of reflection high-energy electron diffraction (RHEED) from the 2×1 missing row reconstruction of the Au(110) surface have been simulated as a function of surface-atom relaxation at different incident glancing angles using the multislice approach with the edge-patching method. The results demonstrate that the diffracted-beam intensity is extremely sensitive to the surface structure; small surface relaxations lead to large amplitude changes,

* To whom all correspondence should be addressed at: Department of Physics, University of Oslo, PO Box 1048, Blindern, 0316 Oslo 3, Norway.

which is consistent with similar claims by previous authors using different methods. The high surface sensitivity of RHEED indicates that it can be used to fingerprint surface relaxations if a reliable simulation tool is available.

I. Introduction

Surface structures, for either clean or adsorbed surfaces, have been mainly investigated by low-energy electron diffraction (LEED). On the other hand, surface structure information has also been successfully obtained using the diffraction of high-energy electrons at glancing incidence (RHEED) in several cases (Menadue, 1972; Ino, 1977, 1980; Gotoh & Ino, 1978). In recent years more attention has been given to RHEED with its successful application to layer-by-layer crystal growth control in molecular beam epitaxy (MBE) facilities (Neave & Joyce, 1983; Van Hove, Lent, Pukite & Cohen, 1983).

Fast electrons in reflection geometry interact mainly with the nucleus of surface atoms, whereas the slow electrons used in LEED interact with both the nucleus and the electrons of surface atoms. It is therefore evident that RHEED intensities are sensitive to surface structures and can be interpreted more readily than LEED. It is especially true for the investigation of surface relaxations which are normal to both the surface and the incident beam in RHEED geometry.

In the theoretical development of RHEED, Collela (1972) and Moon (1972) first extended the n-beam Block-wave dynamical calculation to RHEED problems. Later it was applied to interpret RHEED intensities from the Si(001) surface by Britze & Meyer-Ehmsen (1978) and the effects of surface contraction (or negative relaxation) of the Si(001) surface on RHEED intensities were discussed. Maksym & Beeby (1981) derived a slice method for RHEED problems in which the crystal was sliced parallel to the surface. The results showed that RHEED intensities were sensitive to surface contractions of 5 to 10% in the topmost layer on the Ag(001) surface. A different multislice approach due to Cowley & Moodie (1957, 1959) was applied to RHEED problems by Peng & Cowley (1986), in which the crystal was sliced normal to the surface and incident beam.

Previously, RHEED intensities were found (Ma, 1990; Ma & Marks, 1990a, 1991) to be highly sensitive to the surface termination, $i.e.$ the surface potential modulation normal to the surface and incident beam. This has raised a boundary-matching problem in the n-beam Bloch-wave method (Ma & Marks, 1991). This also implicitly requires the potential sampling rate normal to the surface and the incident beam to be significantly increased in the method of slicing the crystal parallel to the surface and incident beam, otherwise the solution may not be correct (Ma,

1990a, b; Ma & Marks, 1991). The multislice approach (slicing normal to the surface and the incident beam) is a powerful technique for RHEED simulations due to the proliferation of multislice programs and the high sampling rate in the plane normal to the surface and the incident beam. The edge effects of the method, which prevent the method from obtaining a stationary solution, have been overcome by using the edge-patching method (Ma, 1991; Ma & Marks, 1990a, 1991). The current paper seeks to demonstrate that the multislice approach with edge patching can be used for solving one of various RHEED problems, determining surface relaxation using the RHEED technique. The missing row reconstruction of gold, Au(110)–2 × 1, was simulated as a function of the relaxation of reconstructed surface atoms at different incident angles. The results show again that RHEED is highly sensitive to surface relaxations. The different diffracted beams in the resulting RHEED patterns exhibited widely disparate intensity behavior, thus suggesting that surface relaxations or, more generally, all other surface structures may well be identified by these distinguishable RHEED patterns.

II. Numerical method

The multislice approach with edge patching has been discussed in detail elsewhere (Ma, 1991; Ma & Marks, 1991). The method of simulating surface reconstructions in the framework of the multislice method has been presented previously (Ma & Marks, 1990b). Fig. 1(a) shows the complete unit cell with size $4 \times 2^{1/2}a \times 2a$ for the multislice calculation (where a denotes the magnitude of the primitive unit-cell vector of gold). The cell is comprised of $\frac{3}{4}$ vacuum (from A to B) and $\frac{1}{4}$ crystal (from B to C). The 1D profile of the crystal potential for the Au(110) surface in the $[1\bar{1}0]$ zone is shown in Fig. 1(b). For the 2 × 1 reconstruction, the unit cell needs to be two times larger than the primitive vector along (001) and the reconstructed surface atom is positioned as shown in the diagram (Fig. 1a). The high-energy electron reflection from the Au(110)–2 × 1 reconstruction was simulated
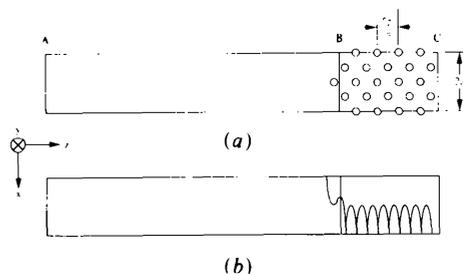
Fig. 1. Diagrams of the complete unit cell with the size $4 \times 2^{1/2}a \times 2a$ for (a) the multislice calculation and (b) the 1D potential profile for the Au(110) surface in the $[1\bar{1}0]$ zone.

under conditions of 50 keV electrons incident upon the (110) surface at 25 and 50 mrad glancing angles to [1$\bar{1}$0] and zero azimuth with respect to the (001) plane. The coordination axes are assigned as the following: x [001]; y [$\bar{1}$10]; z[$\bar{1}\bar{1}$0]; and the incident beam is along the y axis (Fig. 1). Crystal absorption has been taken into account in all subsequent simulations by taking the imaginary component of the crystal potential as 10% of its real component. The outermost surface reconstructed atoms in the simulation were relaxed normal to (110) for both expansion ('positive relaxation') and contraction ('negative relaxation') cases. The relaxation of the topmost reconstructed atoms is defined as the percentage of their corresponding coordinates in the bulk along (110). The calculations were conducted on an Apollo 3500 computer equipped with a Mercury array processor and were imaged by means of the *NUMIS* and *SEMPERVI* routines available at Northwestern University. The stationary solution of the reflected wave was achieved after 1000 iterations of the multislice routines for 25 mrad incidence. The thickness of each iteration Δy is 1·442 Å. Although the calculations for higher glancing angles converged faster than lower angles, 1000 iterations were used in both 25 and 50 mrad incidences for consistency. The RHEED patterns were analyzed for their intensity distributions with a fixed aperture size and all beam maxima were normalized to the incident-beam intensity for comparison.

III. Results and discussions

Fig. 2 illustrates the wave intensity outputs for 50 mrad incidence and 0% relaxation at different thicknesses. The output series are: 1, 100, 200, 300, 400, 500, 600, 800, 1000, 1200 and the total iteration thickness is about 1730 Å. As it indicates, the wave field converges to a stationary solution after about 1000 iterations. The wave field in the crystal (from B to C) decays to zero because of crystal absorption and wave extinction. The periodic boundary conditions imposed by the multislice approach have little effect on the solution because of the wave damping and the zero field imposed at the two ends of the unit cell (A and C). Fig. 3 shows the RHEED patterns at 25 mrad to the [1$\bar{1}$0] for three different relaxations normal to the (110) surface: −10% (inward or contraction) (a), 0% (b) and +10% (outward or expansion) (c), with respect to the bulk positions of those topmost reconstructed atoms. These patterns were obtained by the Fourier transform of the vacuum waves (from A to B) excluding the edge-patching area. Note that the transmitted incident beam is saturated for a clearer display of the Bragg reflections (the ratio between the two is about 10^3–10^4). Experimentally, the transmitted beam is cut off by the edge of the crystal specimen. One can easily notice that different surface relaxations result in dramatic changes in diffracted-beam intensity. For quantitative analysis, the normalized amplitude of each beam is plotted as a function of surface relaxation in Fig. 4 for 25 mrad incidence. Fig. 4(a) is the plot of behavior of the bulk diffracted beams. Here, the (0, 1) and (0, 2) beams correspond to the $\{hh1\}$ and $\{hh2\}$ reflection rods, respectively. While the (0, 1) beam has large intensity variations with relaxation, the (0, 2) beam is only slowly oscillatory. It should be noted that the specularly reflected beam, (0, 0), exhibits behavior similar to the (0, 1) on an even larger scale. Fig. 4(b)
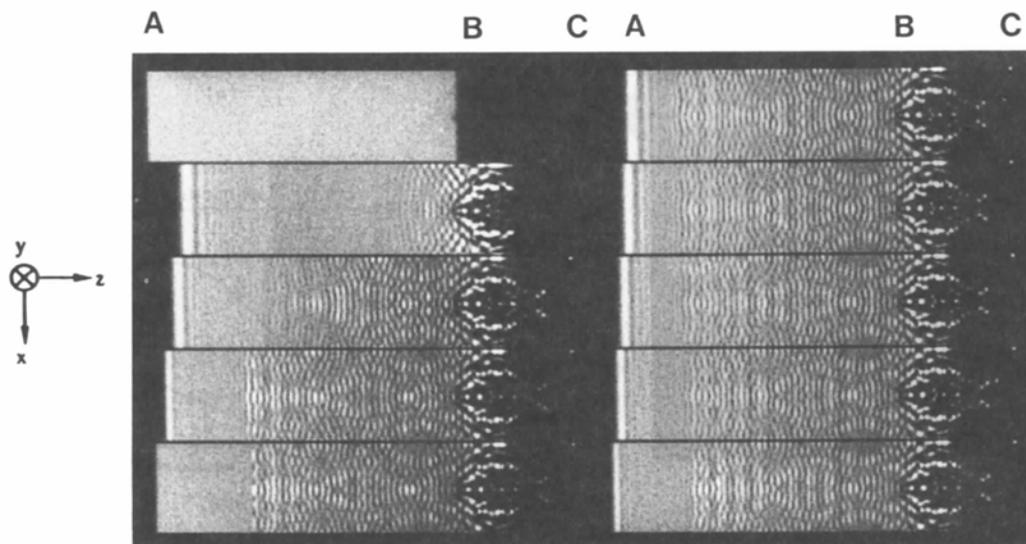
Fig. 2. Wave intensity outputs for 50 mrad incidence and 0% relaxation at different thicknesses. The output series is: 1, 100, 200, 300, 400, 500, 600, 800, 1000, 1200 and the total thickness of the iteration (1200Δy) is 1730 Å. The incident energy is 50 keV and the crystal absorption is 10%.

plots the amplitude oscillations of the beams due to the reconstructed surface as a function of relaxation. Again, while the $(0, \frac{1}{2})$ beam exhibits large fluctuations in amplitude, the $(0, 1\frac{1}{2})$ beam varies only slowly. Fig.

$5(a)$ plots the behavior of the $(0, 0)$ and $(0, 1)$ beams while Fig. $5(b)$ depicts the $(0, 2)$ and $(0, 3)$ beams for 50 mrad incidence. Here, the $(0, 3)$ beam corresponds to the $\{hh3\}$ reflection rods. One rather interesting feature of these plots is that while all four beams exhibit oscillatory behavior, the $(0, 0)$ and $(0, 1)$ beams seem to be 'out of phase' and the $(0, 2)$ and $(0, 3)$ beams oscillate 'in phase'. Similar results are found for the reconstructed surface beams, *i.e.* Figs. $5(c)$ and (d), where $(0, \frac{1}{2})$ and $(0, 1\frac{1}{2})$ beams are 'in phase' while $(0, 2\frac{1}{2})$ and $(0, 3\frac{1}{2})$ beams have suffered a phase shift in oscillation. Here, we have seen an interesting physical phenomenon; the surface reconstructed atoms are redistributing the intensities of the bulk reflection beams and modulating the intensities of all reflection beams as a function of their relaxation distance normal to the surface. The fact that the intensities of RHEED patterns are highly sensitive to the relaxation distance of the topmost atomic surface layer itself indicates that any RHEED calculation must take small-scale potential modulations normal to the surface and the incident beam into account. In other words, it must have a high potential sampling rate normal to the surface which should be less than 1% of the distance between the nearest neighbors in the bulk. This may make any method of slicing crystals

(a)

(b)

(c)

Fig. 3. RHEED patterns at 25 mrad to [1$\bar{1}$0] for three different relaxations normal to the (110) surface: (a) −10%, (b) 0% and (c) +10%. These are the Fourier transforms of the vacuum waves (from A to B indicated in Fig. 1) excluding the edge-patching area.
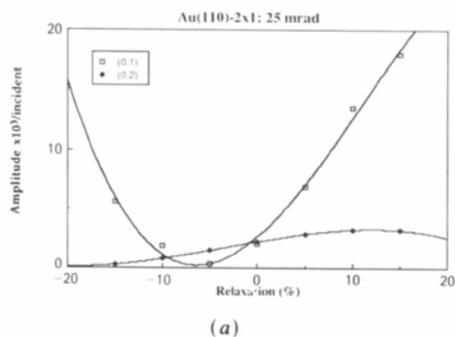
(a)
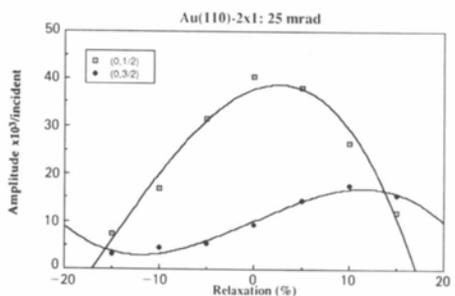
(b)

Fig. 4. Plots of the beam amplitude *vs* relaxation for the bulk diffracted beams (a) $(0, 1)$ and $(0, 2)$ and (b) reconstruction beams $(0, \frac{1}{2})$ and $(0, 1\frac{1}{2})$ for 25 mrad incidence. The data were fit with third-order polynomials.
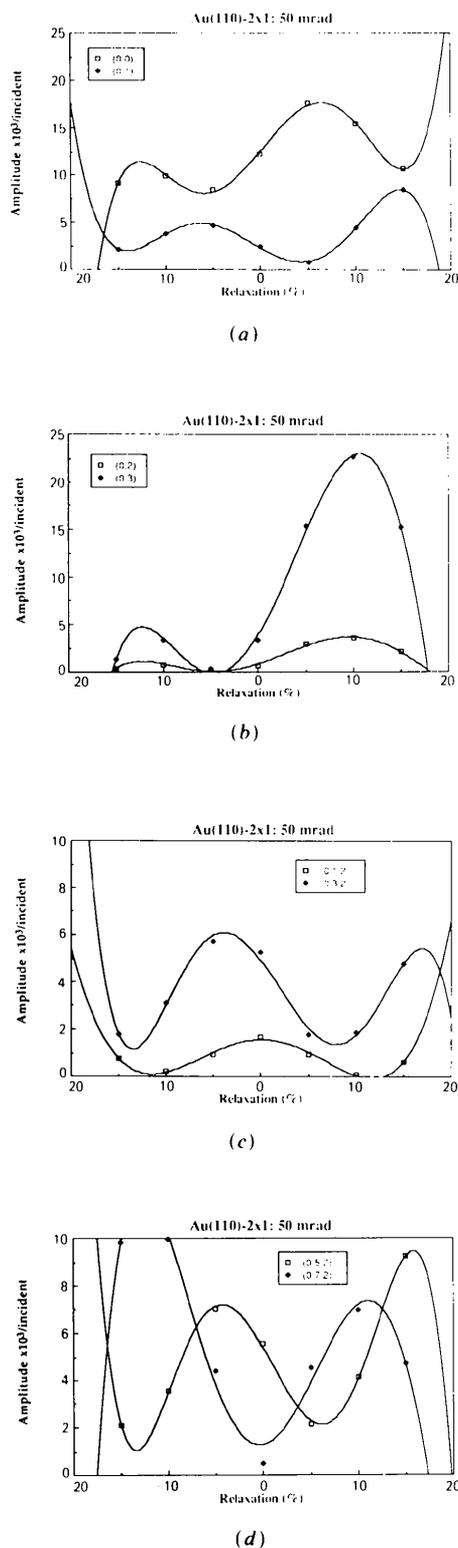
parallel to the surface in RHEED calculations intractable both numerically and economically.

It is important to realize at this point that, while the diffracted beams vary in intensity, the overall intensity remains a constant due to the conservation of energy or current flow. Also the amplitude variations in Figs. 4 and 5 were fitted with nth-order polynomials to demonstrate the functional trends of the intensity variations of different reflected beams. Ideally, a larger number of surface relaxations should have been simulated to 'fill in' the data; however, in the interest of time this was not done (the use of a supercomputer can expedite the calculations) and the RHEED patterns presented here clearly demonstrate the dramatic intensity variations for small values of surface relaxation.

As a summary, it should be pointed out that the simulation of surface reconstructions by means of the edge-patching method in the framework of the multi-slice approach due to Cowley & Moodie (1957, 1959) has shown the possibility of analyzing not only the geometrical spot positions in RHEED patterns but also detailed intensity information. Although we have only conducted the calculation on reconstruction relaxation, the results have demonstrated the ability of the method to calculate a variety of surface structures, which allows more complicated RHEED patterns to be interpreted in a more quantitative way. The dramatic changes in intensity indicate that, in addition to identifying surface reconstructions, the relaxations of individual atoms can be discerned, i.e. each surface and surface reconstruction has its own distinct characteristics different from the others. While the Au(110)-2×1 reconstruction was only treated theoretically here, and has not yet been experimentally verified, the salient point is that it is now possible to calculate the RHEED patterns and identify reconstructions and relaxations from more complicated surfaces.

Fig. 5. Plots of the beam amplitude vs relaxation for the bulk diffracted beams (a) (0,0) and (0,1), (b) (0,2) and (0,3) and reconstruction beams (c) (0,½) and (0,1½), (d) (0,2½) and (0,3½) for 50 mrad incidence. The data were fit with fifth-order polynomials.

References

BRITZE, K. & MEYER-EHMSEN, G. (1978). Surf. Sci. 77, 131-141.
COLELLA, R. (1972). Acta Cryst. A28, 11-15.
COWLEY, J. M. & MOODIE, A. F. (1957). Acta Cryst. 10, 609-619.
COWLEY, J. M. & MOODIE, A. F. (1959). Acta Cryst. 12, 353-359.
GOTOH, Y. & INO, S. (1978). J. Appl. Phys. Jpn, 17, 2097-2109.
INO, S. (1977). Jpn. J. Appl. Phys. 16, 891-908.
INO, S. (1980). Jpn. J. Appl. Phys. 19, 1277-1290.
MA, Y. (1990). Proc. of the XII International Congress for Electron Microscopy, Vol. 2, pp. 374-375.
MA, Y. (1991). Acta Cryst. A47, 137-139.
MA, Y. & MARKS, L. D. (1990a). J. Electron Microsc. Tech. In the press.
MA, Y. & MARKS, L. D. (1990b). Acta Cryst. A46, 594-606.

MA, Y. & MARKS, L. D. (1991). *Acta Cryst.* A47, 707-715.
MAKSYM, P. A. & BEEBY, J. L. (1981). *Surf. Sci.* 110, 423-436.
MENADUE, J. F. (1972). *Acta Cryst.* A28, 1-11.
MOON, A. R. (1972). *Z. Naturforsch. Teil A*, 390-395.

NEAVE, J. H. & JOYCE, B. A. (1983). *Appl. Phys.* A31, 1-8.
PENG, L. M. & COWLEY, J. M. (1986). *Acta Cryst.* A42, 545-552.
VAN HOVE, J. M., LENT, C. S., PUKITE, P. R. & COHEN, P. I. (1983). *J. Vac. Sci. Technol.* B1(3), 741-746.

Low-Resolution Phases: Influence on SIR Syntheses and Retrieval with Double-Step Filtration

BY A. G. URZHUMTSEV

Research Computer Centre, Academy of Sciences of the USSR, Pushchino, Moscow Region, 142292 USSR

Abstract

Different sources of error in single isomorphous replacement (SIR) maps are analysed. It is shown that SIR maps are good enough in themselves to localize a molecule but the absence of low-resolution reflections can distort the image of the molecule. Even in this case the molecule can be reliably localized using the double-step filtration technique of Urzhumtsev, Lunin & Luzyanina [*Acta Cryst.* (1989), A45, 34-39] if parameters are chosen appropriately. On the other hand, such syntheses may be considerably improved by addition of low-resolution structure factors. A very simple procedure is suggested to retrieve unknown phases for these structure factors.

I. Introduction

At the beginning of a macromolecular structure determination, electron density syntheses may be so noisy that the molecules cannot be localized. Different sources of errors influence synthesis distortions. Some of them have recently been analysed by Fenderson, Herriott & Adman (1990). In our work we have analysed the influence of some other sources of synthesis errors: using isomorphous replacement phases instead of the exact values and lack of very low-resolution reflections in the synthesis (loss of the central zone of reciprocal space).

Earlier, Podjarny, Schevitz & Sigler (1981) and Luzzatti, Mariani & Delacroix (1988) noted the significance of low-resolution phases. Now we have succeeded in both qualitative and quantitative estimation of the effect of these omitted reflections. This omission was shown to be the main cause of molecular image distortion. Unfortunately, determination of the corresponding phases by the isomorphous replacement method is problematic, in particular because of the well known disordered solvent contribution.

When molecule boundaries can be found, the powerful solvent-flattening procedure (Bricogne, 1974) may be used to improve the synthesis. To localize a molecule in a very noisy synthesis, similar procedures were independently developed by Stuart (1988), Urzhumtsev (1985), Wang (1985) and Westbrook (see, Podjarny, Moras, Navaza & Alzari, 1988). The most popular of these approaches is the Wang (1985) procedure. This was successfully inserted into the general density-modification scheme (Podjarny, 1987) which was used from the beginnings of protein crystallography (see *e.g.* Qurashi, 1953).

There is a widespread point of view that the basis of the Wang procedure is a local averaging of a noisy synthesis. However, as was shown by Urzhumtsev *et al.* (1989), the averaging by itself does not produce molecule boundaries and the key point is the preliminary nonlinear filtration of the synthesis. In the Wang procedure this step is carried out indirectly by calculating the synthesis without F_{000}/V and removing negative density. Wang has not paid due attention to this step although the results for molecular boundaries depend on its parameters (Urzhumsev *et al.*, 1989). We have demonstrated that the appropriate choice of parameters for both nonlinear filtration and averaging enables one to localize the molecule even in a very noisy synthesis, in particular, one calculated without low-resolution reflections.

When low-resolution reflections are unphased the synthesis may also be improved by phase extension to the low-resolution region which is the exact opposite to the usual phase extension to high-resolution reflections. Some authors working with viruses structures in particular include these reflections in synthesis calculations, obtaining the phases from a model (*e.g.* Harrison & Jack, 1975). This situation differs from the one discussed here where a model is absent but more high-resolution phases are known, maybe with some errors. Earlier, Podjarny *et al.*